Archives of Toxicology (2021) 95:135–148
https://doi.org/10.1007/s00204-020-02894-0

MOLECULAR TOXICOLOGY

Clioquinol inhibits dopamine-β-hydroxylase secretion and noradrenaline synthesis by affecting the redox status of ATOX1 and copper transport in human neuroblastoma SH-SY5Y cells

Masato Katsuyama[1] · En Kimura[2] · Masakazu Ibi[3] · Kazumi Iwata[3] · Misaki Matsumoto[3] · Nozomi Asaoka[3] · Chihiro Yabe-Nishimura[3]

Received: 24 April 2020 / Accepted: 27 August 2020 / Published online: 9 October 2020

Abstract

Clioquinol (5-chloro-7-indo-8-quinolinol), a chelator and ionophore of copper/zinc, was extensively used as an amebicide to treat indigestion and diarrhea in the mid-1900s. However, it was withdrawn from the market in Japan because its use was epidemiologically linked to an increase in the incidence of subacute myelo-optic neuropathy (SMON). SMON is characterized by the subacute onset of sensory and motor disturbances in the lower extremities with occasional visual impairments, which are preceded by abdominal symptoms. Although pathological studies demonstrated axonopathy of the spinal cord and optic nerves, the underlying mechanisms of clioquinol toxicity have not been elucidated in detail. In the present study, a reporter assay revealed that clioquinol (20–50 μM) activated metal response element-dependent transcription in human neuroblastoma SH-SY5Y cells. Clioquinol significantly increased the cellular level of zinc within 1 h, suggesting zinc influx due to its ionophore effects. On the other hand, clioquinol (20–50 μM) significantly increased the cellular level of copper within 24 h. Clioquinol (50 μM) induced the oxidation of the copper chaperone antioxidant 1 (ATOX1), suggesting its inactivation and inhibition of copper transport. The secretion of dopamine-β-hydroxylase (DBH) and lysyl oxidase, both of which are copper-dependent enzymes, was altered by clioquinol (20–50 μM). Noradrenaline levels were reduced by clioquinol (20–50 μM). Disruption of the *ATOX1* gene suppressed the secretion of DBH. This study suggested that the disturbance of cellular copper transport by the inactivation of ATOX1 is one of the mechanisms involved in clioquinol-induced neurotoxicity in SMON.

Keywords Clioquinol · SMON · ATOX1 · Dopamine-β-hydroxylase

Introduction

Clioquinol (5-chloro-7-indo-8-quinolinol) was used extensively as an amebicide to treat indigestion and diarrhea in the mid-1900s. However, it was withdrawn from the market in Japan because its use was epidemiologically linked to an increase in the incidence of subacute myelo-optic neuropathy (SMON) (Tsubaki et al. 1971). SMON is characterized by the subacute onset of sensory and motor disturbances in the lower extremities with occasional visual impairments, which are preceded by abdominal symptoms (Nakae et al. 1973; Tsubaki et al. 1971). Although pathological studies demonstrated axonopathy of the spinal cord and optic nerves (Tateishi 2000), the underlying mechanisms of clioquinol toxicity have not been elucidated in detail (Asakura et al. 2009; Benvenisti-Zarom et al. 2005; Cater and Haupt 2011; Fukui et al. 2015; Kawamura et al. 2014; Mao et al. 2009).

Electronic supplementary material The online version of this article (https://doi.org/10.1007/s00204-020-02894-0) contains supplementary material, which is available to authorized users.

✉ Masato Katsuyama
mkatsuya@koto.kpu-m.ac.jp

[1] Radioisotope Center,, Kyoto Prefectural University of Medicine, 465 Kajii-cho, Kamigyo-ku, Kyoto 602-8566, Japan

[2] Department of Clinical Research Support, Translational Medical Center, National Center of Neurology and Psychiatry, Kodaira 187-8551, Japan

[3] Department of Pharmacology, Kyoto Prefectural University of Medicine, Kyoto 602-8566, Japan

To clarify the molecular mechanisms underlying clioquinol-induced neurotoxicity, we previously performed a global analysis of human neuroblastoma cells using DNA chips (GEO database accession code: GSE32173) and demonstrated that clioquinol induced DNA double-strand breaks, leading to the activation of ATM and downstream p53 signaling (Katsuyama et al. 2012). This pathway may, at least in part, function in clioquinol-induced neurotoxicity. We also found that clioquinol induced the expression of VGF, the precursor of neuropeptides involved in pain reactions, by inducing c-Fos, one of the activator protein-1 transcription factors (Katsuyama et al. 2014). The induction of VGF suggests its involvement in clioquinol-induced mechanical hyperalgesia and cold allodynia (Andersson et al. 2009). We also reported that clioquinol induced the expression of interleukin-8 (IL-8), a key chemokine responsible for the activation and recruitment of neutrophils to sites of inflammation, by down-regulating GATA-2 and GATA-3 (Katsuyama et al. 2018). The induction of IL-8 expression suggests its involvement not only in the initial symptoms of SMON, such as abdominal pain and/or diarrhea, but also in subsequent dysesthesia or optic neuritis.

Clioquinol has been used as a therapeutic agent for acrodermatitis enteropathica, a disorder of dietary zinc absorption caused by mutations in the gene encoding ZIP4 (SLC39A4), a zinc importer (Kury et al. 2002; Sturtevant 1980). The therapeutic effects of clioquinol are attributable to its characteristics as a zinc ionophore because it was previously demonstrated to alter the effects of zinc supplementation in a mouse model of acrodermatitis enteropathica (Geiser et al. 2013). On the other hand, some cases of neuropathy are caused by high zinc levels and copper deficiency. Myelo-optic neuropathy related to acquired copper deficiency was previously reported in a patient who underwent partial gastrectomy (Spinazzi et al. 2007). The use of denture cream containing excess zinc also resulted in copper deficiency and myelopolyneuropathy (Hedera et al. 2003, 2009; Nations et al. 2008). Furthermore, several common features were identified among clinical symptoms and neuroanatomical focal distributions between SMON and myeloneuropathy caused by copper deficiency (Kimura et al. 2011). This suggests that SMON is a neuropathy caused by copper deficiency due to excessive zinc intake.

According to the global analysis, clioquinol markedly increased the expression levels of several metallothioneins, suggesting the influx of metal ions. As clioquinol functions as a chelator of copper/zinc and their ionophores, we focused on the alteration of copper/zinc homeostasis in cells by clioquinol. We demonstrated that clioquinol induced the oxidation of the copper chaperone antioxidant 1 (ATOX1), altered the secretion of dopamine-β-hydroxylase (DBH), a copper-dependent ectoenzyme involved in the biosynthesis of noradrenaline (NA), and reduced the cellular NA level.

Materials and methods

Materials

Clioquinol was purchased from Merck (Darmstadt, Germany). Antibodies against ATOX1 [EPR10352] and lysyl oxidase (LOX) [EPR4025] were purchased from Abcam (Cambridge, UK). The antibody against DBH was purchased from Cell Signaling Technology (Danvers, MA). The antibody against β-actin (6D1) was obtained from Medical and Biological Laboratories (Nagoya, Japan).

Cell culture

Human neuroblastoma SH-SY5Y cells, which are frequently used as an in vitro model to examine neurotoxicity (Cheung et al. 2009; Xie et al. 2010), were purchased from the European Collection of Cell Cultures and cultured in Ham's F12: Eagle's medium with Earle's salts (1:1) supplemented with non-essential amino acids and 15% fetal bovine serum (FBS). Unless otherwise noted, these undifferentiated cells were used for analyses. For differentiation to a noradrenergic phenotype, cells were cultured for 3 days in Neurobasal medium (Thermo Fisher Scientific, Waltham, MA) containing B-27 supplement minus antioxidant (Thermo Fisher Scientific) and 1 mM dibutyryl cyclic AMP (dbcAMP) (FUJIFILM Wako Pure Chemical, Osaka, Japan) as described previously (Kume et al. 2008). Clioquinol dissolved in DMSO was added to the culture medium at 1/1000 v/v. As a control, DMSO was added at 1/1000 v/v.

Measurement of metal response element (MRE)-dependent transcriptional activity by luciferase assay

SH-SY5Y cells were seeded on 24-well plates at 1×10^5 cells/well and grown for 24 h. The firefly luciferase vector pGL4.40[luc2P/MRE/Hygro] or pGL4.27[luc2P/minP/Hygro] (0.5 μg/well; Promega, Madison, WI) and Renilla luciferase vector pGL4.74[hRluc/TK] (0.05 μg/well; Promega) were co-transfected with TransIT-LT1 Reagent (Mirus Bio, Madison, WI). These cells were cultured for 24 h and then stimulated with clioquinol for 3 h. Firefly luciferase activity in cell lysates was assessed and normalized to Renilla luciferase activity.

Measurement of intracellular copper and zinc levels

Cells cultured in 6-well plates were washed twice with phosphate-buffered saline (PBS) and lysed in buffer (50 μl) containing 1% Triton, 0.5% sodium deoxycholate, 0.008%

sodium dodecyl sulfate (SDS), 10 mM TrisHCl (pH 6.8), and 150 mM NaCl. The lysate was centrifuged and the protein concentration of the supernatant was measured. After the addition of 6 N HCl (0.5 µl) to liberate metal ions chelated by proteins, copper (Cu^{2+} and Cu^{+}) and zinc (Zn^{2+}) levels were measured using the Metallo Assay LS kit (Metallogenics, Chiba, Japan).

Monitoring of the redox status of ATOX1

The redox status of ATOX1 was monitored using -Sulfo-Biotics- Protein Redox State Monitoring Kit Plus (Dojindo Molecular Technologies, Kumamoto, Japan). Cells were washed twice with PBS and lysed in buffer containing 1% Triton, 0.5% sodium deoxycholate, 10 mM TrisHCl (pH 6.8), 150 mM NaCl, 1 mM EDTA, protease inhibitor cocktail (Nacalai Tesque, Kyoto, Japan), 1 mM NaF, and 1 mM Na_3VO_4. The lysate was centrifuged and the supernatant was used as whole cell lysate. Aliquots containing equal amounts of protein (2 µg) were labeled with DNA-maleimide according to the manufacturer's instructions and then separated on 15% SDS–polyacrylamide gels with a molecular size marker (Precision Plus Dual Standard, Bio-Rad, Tokyo, Japan). To detect total ATOX1, the whole cell lysate (2 µg) was applied to the same gels. Gels were irradiated with UV to remove DNA before their transfer onto polyvinylidene difluoride membranes (Merck). Western blotting was performed as described previously (Katsuyama et al. 2018).

Quantitative PCR

Quantitative PCR was performed as described previously (Katsuyama et al. 2012). Cells were seeded on 6-well plates (5×10^5 cells/well), cultured for 24 h, and then stimulated with clioquinol. Gene expression was quantified using standard curves that were generated using serially diluted plasmid reference samples and normalized to the expression level of hypoxanthine phosphoribosyltransferase (HPRT). The specificities of PCR products were confirmed by gel electrophoresis and dissociation curve analysis. The sequences of the primers used to detect DBH and LOX were as follows: 5′-TACTGCACGGACAAGTGCACCCAG-3′ (DBH sense), 5′-GTTGTACGTGCAGGAGGTGATGAG-3′ (DBH antisense), 5′-ACTATGGCTACCACAGGCGATT-3′ (LOX sense), and 5′-AGCTGGGGTTTACACTGACCTT-3′ (LOX antisense). The sequences of the primers used to detect HPRT were described previously (Katsuyama et al. 2018).

Detection of DBH and LOX secreted into culture media

Cells were cultured in 6-cm dishes in the presence or absence of clioquinol for 24 h. After washing with PBS, cells were cultured for 8 h with serum-free medium containing the same concentration of clioquinol. Media were collected and cell debris was removed by centrifugation. Concentration and desalting were performed using a centrifugal filter (Amicon Ultra-4, 10 kDa cut-off, Merck). Whole cell lysates were prepared as described above after the removal of media and washing with PBS. Western blotting was performed as described previously (Katsuyama et al. 2018).

Measurement of the NA level

Cells were cultured in 6-cm dishes in the presence or absence of clioquinol for 24 h. After washing with PBS, cells were harvested and sonicated in a solution containing 0.01 N HCl, 1 mM EDTA, and 4 mM $Na_2S_2O_5$. After centrifugation, supernatants were used as NA extracts and subjected to protein concentration measurement. The intracellular level of NA was measured using the Noradrenaline Research ELISA kit according to the manufacturer's protocol (ImmuSmol, Bordeaux, France).

Genome editing of ATOX1

Genome editing of ATOX1 was performed by transfecting the nickase expression vector AIO-puro (Addgene, Cambridge, MA). Guide RNA (gRNA) sequences against the human *ATOX1* gene were designed by CRISPRdirect (https://crispr.dbcls.jp). The sense sequences of gRNA were 5′-AGCUUCAGCACAGCCUCCAC-3′ and 5′-UCUCGGGUCCUCAAUAAGCU-3′. Oligonucleotides corresponding to the gRNA sequence were inserted into AIO-puro and the vector was transfected into SH-SY5Y cells by electroporation using the 4D-Nucleofector System (Lonza, Basel, Switzerland). Stable transfectants were selected by single-cell cloning in the presence of puromycin (5 µg/ml). Regarding mock transfection, the AIO-puro vector was transfected and selected with puromycin. The disruption of ATOX1 was confirmed by Western blotting.

Statistical analysis

Values were expressed as the mean ± SE. After testing the homogeneity of variance, statistical analyses were performed using the Student's *t*-test. One-way ANOVA followed by Bonferroni's *t*-test was applied to multiple treatment groups. *P* values less than 0.05 were considered to be significant.

Results

Clioquinol induced zinc influx

Clioquinol is conventionally recognized as a copper/zinc chelator (Cherny et al. 2001; Choi et al. 2006). However, it

also functions as a copper/zinc ionophore that brings these metal ions into cells (Andersson et al. 2009; Ding et al. 2005). To clarify whether clioquinol affects intracellular copper/zinc levels, we focused on the expression of genes that may be affected by these metal ions. In the global analysis of human neuroblastoma SH-SY5Y cells using DNA chips, stimulation with 50 µM clioquinol for 24 h markedly increased the expression of metallothioneins (MT), a family of metal-binding proteins (GEO database accession code: GSE32173) (Katsuyama et al. 2012). Among 4 MT isoforms, 7 subclasses of MT-1 and MT-2A were strongly up-regulated by clioquinol. It also induced the up-regulation of SLC30A1 (zinc exporter ZnT1), suggesting that it activated metal regulatory transcription factor 1 (MTF1)-dependent transcription (Grzywacz et al. 2015; Langmade et al. 2000). As shown in Fig. 1a, stimulation with clioquinol for 3 h significantly activated MRE-dependent transcription at concentrations of 20 µM and higher, demonstrating that clioquinol increased the intracellular metal concentration.

We then examined clioquinol-induced changes in intracellular copper/zinc levels. As shown in Fig. 1b, stimulation with 50 µM clioquinol for 1 h significantly increased the intracellular zinc level. On the other hand, clioquinol alone did not increase the intracellular level of copper, but induced marked increases in the presence of 50 µM $CuCl_2$ (Fig. 1c). This suggests that the clioquinol-induced activation of MRE-dependent transcription is mediated by zinc influx.

Clioquinol induced the intracellular accumulation of copper

To investigate whether clioquinol affects copper metabolism, clioquinol-induced changes in the intracellular level of copper were examined up to 24 h. As shown in Fig. 2a, 50 µM clioquinol induced a significant increase in the intracellular level of copper within 24 h. This increase was observed at concentrations of 20 µM and higher (Fig. 2b). In contrast to the influx of zinc within 1 h, the increase in the copper level within 24 h suggested that clioquinol causes the accumulation of copper rather than its influx.

Clioquinol induced the oxidation of ATOX1

ATOX1 is a copper chaperone that transfers cytosolic copper to ATP7A and ATP7B, which are copper-transporting ATPases localized in the membranes of the trans-Golgi network (TGN) and vesicles, respectively (Schmidt et al. 2018). It was originally identified in yeast and named after its characteristic of protecting superoxide dismutase (SOD)-deficient yeast from oxidative damage (Lin and Culotta 1995). ATOX1 was also demonstrated to promote neuronal survival (Kelner et al. 2000) and copper flow regulated by

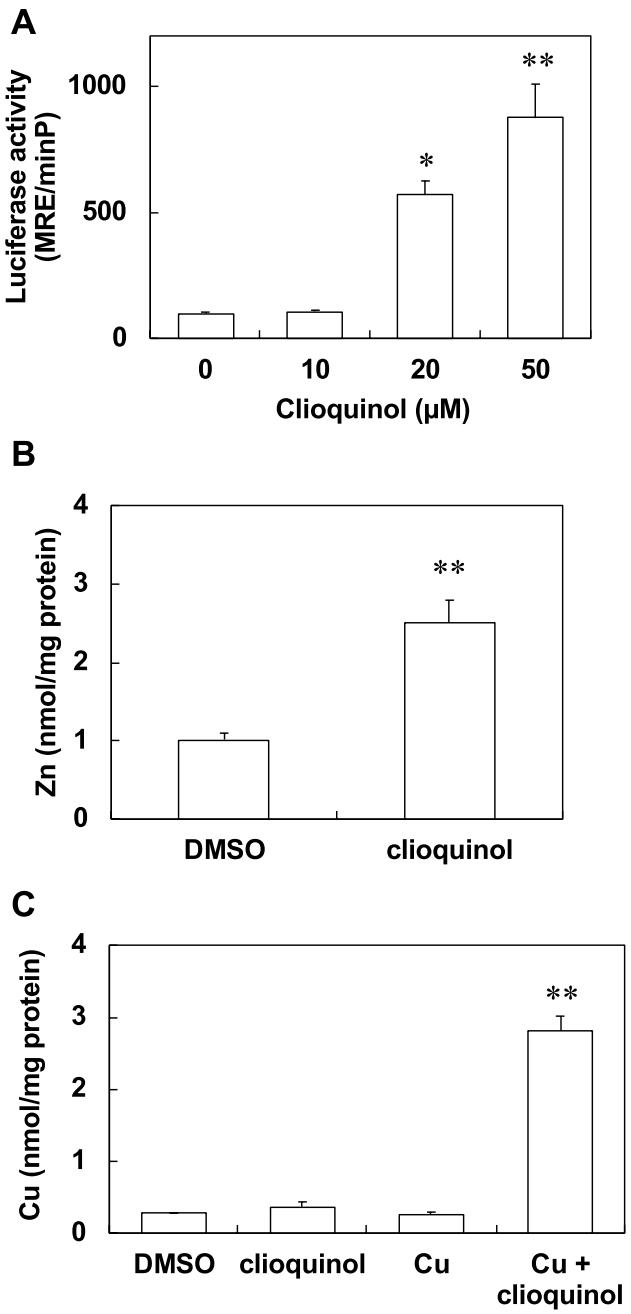

Fig. 1 Clioquinol increased the intracellular level of zinc within 1 h. **a** Clioquinol induced metal response element (MRE)-dependent transcriptional activation. The firefly luciferase vector pGL4.40 (MRE) or pGL4.27 (minP) and Renilla luciferase vector pGL4.74 were co-transfected into SH-SY5Y cells. Cells were cultured for 24 h and then stimulated with the indicated concentration of clioquinol for 3 h. Firefly luciferase activity in cell lysates was assessed and normalized to that of Renilla luciferase activity. Bars represent the means ± SE of 3 experiments. *$p < 0.05$, **$p < 0.01$ vs. 0 µM. **b** Clioquinol increased the intracellular level of zinc. SH-SY5Y cells were stimulated with 50 µM clioquinol for 1 h, and the intracellular level of zinc was measured as described in "Materials and methods" section. Bars represent the means ± SE of four individual wells. **$p < 0.01$ vs. DMSO. **c** Clioquinol did not increase the intracellular level of copper in the absence of an excess amount of extracellular copper. SH-SY5Y cells were stimulated with 50 µM clioquinol for 1 h in the presence or absence of 50 µM $CuCl_2$, and the intracellular level of copper was measured as described in "Materials and methods" section. Bars represent the means ± SE of four individual wells. **$p < 0.01$ vs. DMSO

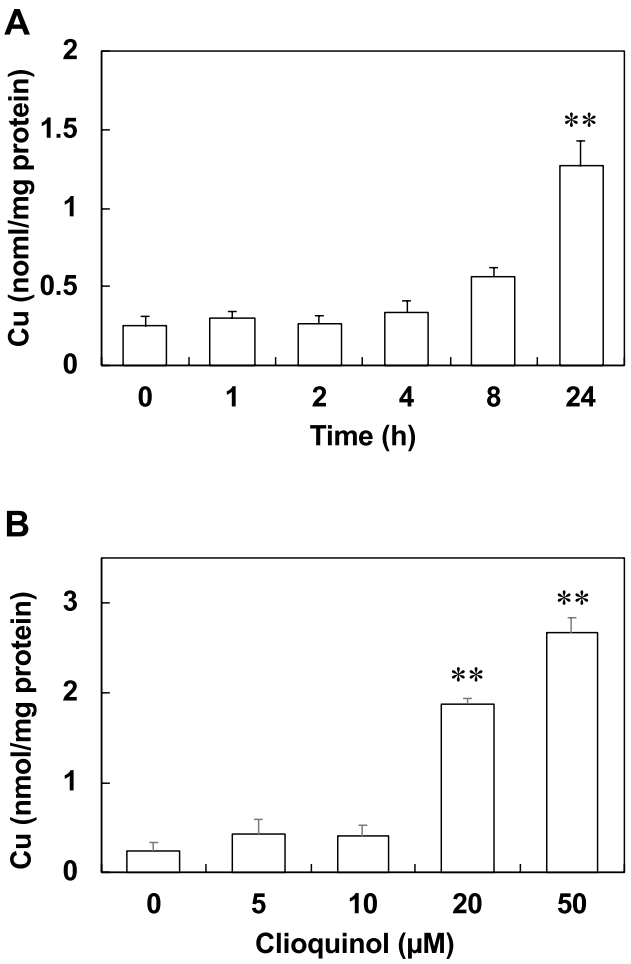

Fig. 2 Clioquinol increased the intracellular level of copper within 24 h. **a** Time course of clioquinol-induced increases in the intracellular level of copper. Cells were grown in the presence of 50 μM clioquinol for the indicated time. Bars represent the means ± SE of four individual wells. $^{**}p < 0.01$ vs. 0 h. **b** Dose-dependent increases in the intracellular level of copper. Cells were grown in the presence of the indicated concentrations of clioquinol for 24 h. Bars represent the means ± SE of four individual wells. $^{**}p < 0.01$ vs. 0 μM

its redox status is associated with neuronal differentiation (Hatori et al. 2016). The oxidation of ATOX1 at the metal-binding motif was suggested to disturb its copper-delivering function. As clioquinol induces oxidative stress (Kawamura et al. 2014), we examined whether it affected the redox status of ATOX1. Three cysteine residues are present in human ATOX1 (MW = 7.4 kDa), two of which are within the metal-binding motif (MXCXXC). All three cysteine residues exist as free thiols in the reduced form, whereas a disulfide bond is formed within the metal-binding motif in the oxidized form. By labeling free thiols with DNA-maleimide, clioquinol-induced changes in the redox status of ATOX1 were monitored. ATOX1 was detected as a band of approximately 7 kDa using conventional Western blotting. Clioquinol did not affect the protein levels of total ATOX1 (Fig. 3a, left four lanes). Labeling with DNA maleimide yielded two bands at approximately 17 and 45 kDa, corresponding to the oxidized form (labeled at one thiol) and reduced form (labeled at 3 thiols), respectively. The band for the reduced form disappeared following stimulation of the cells with 50 μM clioquinol for 24 h (Fig. 3a). The time-course experiment revealed that clioquinol induced the oxidation of ATOX1 within 4 h (Fig. 3b). This suggested that the clioquinol-induced increases in the copper level were due to the oxidation of ATOX1 and resulting impairment of copper transport.

Clioquinol inhibited the secretion of copper ectoenzymes

Impairment of copper transport disturbs the activation and secretion of copper-dependent ectoenzymes such as DBH and LOX. Quantitative PCR revealed that DBH mRNA levels were significantly increased by clioquinol at concentrations of 20 μM and higher. On the other hand, LOX mRNA levels were markedly increased by stimulation with 50 μM clioquinol (Fig. 4a). As shown in Fig. 4b, DBH protein levels slightly decreased in cell lysates treated with 50 μM clioquinol. DBH was detected in whole cell lysates and media in the absence of clioquinol, but not in media prepared from cells stimulated with 50 μM clioquinol, suggesting that clioquinol suppressed the secretion of DBH into media. LOX was detected as a proenzyme at approximately 50 kDa in whole cell lysates and as the mature form at 32 kDa in media in the absence of clioquinol, as reported previously (Trackman et al. 1992). Although clioquinol increased LOX proenzyme levels in whole cell lysates, the mature form was not detected in media, suggesting that clioquinol suppressed its secretion. As shown in Fig. 4c, clioquinol suppressed the secretion of DBH at concentrations of 20 μM and higher.

Clioquinol reduced the cellular NA level

DBH is the enzyme that converts dopamine to NA. To examine whether clioquinol inhibits the biosynthesis of NA, the intracellular level of NA was measured by ELISA. As shown in Fig. 4d, clioquinol reduced the cellular level of NA at concentrations of 20 μM and higher in both undifferentiated cells and dbcAMP-induced differentiated cells.

Genome editing of ATOX1 suppressed the secretion of DBH

Genome editing of *ATOX1* was performed to assess whether the oxidation of and functional impairment of ATOX1 play a role in the inhibition of DBH secretion. As shown in Fig. 5, gene disruption of ATOX1 suppressed the secretion of DBH into media, suggesting that the clioquinol-induced inhibition

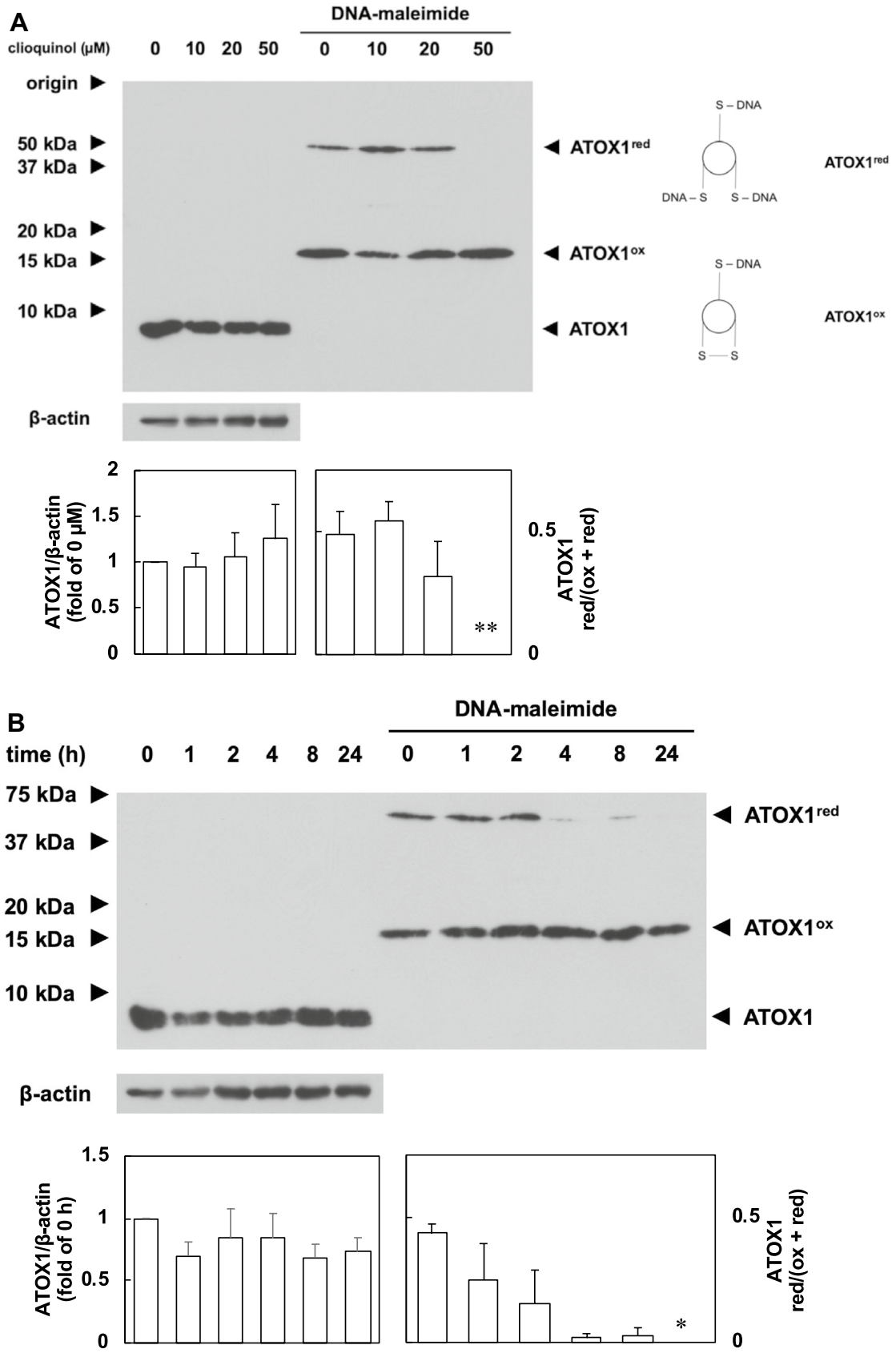
A
DNA-maleimide
clioquinol (μM)
0 10 20 50 0 10 20 50
origin
50 kDa
37 kDa
20 kDa
15 kDa
10 kDa
ATOX1red
ATOX1ox
ATOX1
S – DNA
DNA – S
S – DNA
ATOX1red
S – DNA
S — S
ATOX1ox
β-actin
ATOX1/β-actin (fold of 0 μM)
2
1.5
1
0.5
0
**
0.5
0
ATOX1 red/(ox + red)
B
DNA-maleimide
time (h)
0 1 2 4 8 24 0 1 2 4 8 24
75 kDa
37 kDa
20 kDa
15 kDa
10 kDa
ATOX1red
ATOX1ox
ATOX1
β-actin
ATOX1/β-actin (fold of 0 h)
1.5
1
0.5
0
*
0.5
0
ATOX1 red/(ox + red)

◂**Fig. 3** Clioquinol induced the oxidation of ATOX1. a Dose-dependent decreases in reduced ATOX1. Cells were grown in the presence of the indicated concentrations of clioquinol for 24 h. **b** Time course of clioquinol-induced decreases in reduced ATOX1. Cells were grown in the presence of 50 μM clioquinol for the indicated time. The whole cell lysate (2 μg) was labeled with DNA-maleimide and separated on SDS–polyacrylamide gels. To detect total ATOX1, the whole cell lysate (2 μg) was also applied to the same gels. Western blotting was performed as described in "Materials and methods" section. Reduced ($ATOX1^{red}$) and oxidized ATOX1 ($ATOX1^{ox}$) labeled with DNA-maleimide are shown in the right panel of *A*. The experiment was repeated 3 times and representative results are shown. Quantitation results using ImageJ software are shown as a graph

of DBH secretion was due to the oxidation and functional impairment of ATOX1.

Cytotoxic effects of clioquinol on differentiated SH-SY5Y cells

We examined the cytotoxicity of clioquinol in dbcAMP-induced differentiated SH-SY5Y cells, a model of noradrenergic neurons (Kume et al. 2008). When cells were stimulated with 1 mM dbcAMP for 3 days, prominent neurite elongation and branches were observed (Fig. 6a). As shown in Fig. 6b, clioquinol exerted toxic effects at concentrations of 20 μM and higher, suggesting that the susceptibility of differentiated SH-SY5Y cells to clioquinol is the same as that of undifferentiated cells (Katsuyama et al. 2012).

Discussion

The main results of the present study were as follows: (1) clioquinol activated MRE-dependent transcription; (2) clioquinol increased the total zinc level within 1 h; (3) clioquinol increased the total copper level within 24 h; (4) clioquinol induced the oxidation of the copper chaperone ATOX1; (5) clioquinol disturbed the secretion of the copper-dependent enzymes DBH and LOX; (6) clioquinol reduced the cellular level of NA; and (7) disruption of the *ATOX1* gene suppressed the secretion of DBH. Copper-induced oxidative stress was previously reported to promote zinc-induced neuronal cell death through activation of the stress-activated protein kinase/c-Jun amino-terminal kinase (SAPK/JNK) and a subsequent increase in endoplasmic reticulum (ER) stress (Tanaka et al. 2019). Our study suggested that clioquinol activates these pathways to elicit neuronal cell death. Indeed, our previous global analysis using DNA chips demonstrated that clioquinol markedly increased the expression of CHOP mRNA, a marker of ER stress (GEO database accession code: GSE32173) (Katsuyama et al. 2012). Furthermore, disturbed maturation of copper-dependent ectoenzymes by clioquinol may lead to neuronal dysfunction. Thus, our study suggests that the disturbance of cellular copper transport by the inactivation of ATOX1 is one of the mechanisms involved in clioquinol-induced neurotoxicity in SMON (Fig. 7).

The toxicity of clioquinol was previously observed at concentrations of 20 μM and higher in SH-SY5Y cells (Katsuyama et al. 2012; Kawamura et al. 2014). In the present study, clioquinol-induced MRE-dependent transcriptional activation and copper accumulation were also observed at concentrations of 20 μM and higher. As reported previously, SMON patients were typically administered clioquinol at approximately 1.5 g/day (Egashira and Matsuyama 1982). In human subjects, the single oral intake of 1.5 g of clioquinol resulted in peak plasma concentrations of approximately 20 μg/ml (65 μM) after 4 h, whereas multiple doses (3×0.5 g/day, 3 days) led to a plasma concentration of 30 μg/ml (98 μM) (Jack and Riess 1973). Thus, the concentration of clioquinol used in the present study was similar to the plasma level in SMON patients; however, it currently remains unclear whether affected neurons were exposed to this concentration of clioquinol. In a dog model, clioquinol accumulated and remained in the lumbar cord and sciatic nerve at higher levels than in the liver and kidney even at 9 weeks after withdrawal (Matsuki et al. 1987). Thus, clioquinol may accumulate in neuronal tissues via unknown mechanisms.

Although it was withdrawn from the market, clioquinol and its derivative PBT2 have potential as therapeutics for Alzheimer's disease due to their metal protein-attenuating functions (Bareggi and Cornelli 2012; Faux et al. 2010; Lannfelt et al. 2008; Ritchie et al. 2003). Furthermore, another derivative, PBT434 (Finkelstein et al. 2017), is expected to become an orphan drug for the treatment of multiple system atrophy. Therefore, the present study in combination with previous reports (Asakura et al. 2009; Benvenisti-Zarom et al. 2005; Fukui et al. 2015; Kawamura et al. 2014) warn against the clinical reuse of clioquinol and application of its derivatives.

Although clioquinol is a copper/zinc ionophore, it increased the intracellular level of zinc, but not copper, alone (Fig. 1b, c). Free copper and zinc levels in culture media were 1.50 ± 0.13 μM and 13.02 ± 0.27 μM, respectively ($N = 4$, data not shown). Thus, clioquinol-induced zinc influx was due to the higher concentration of zinc in media than that of copper. Serum copper and zinc levels in a healthy adult range between 70 ~ 130 μg/dL (11 ~ 20 μM) and 80 ~ 130 μg/dL (12 ~ 20 μM), respectively. However, approximately 95% of serum copper is bound to ceruloplasmin, suggesting that free serum copper levels are one-tenth of those of zinc. Thus, copper/zinc levels in our culture system were similar to those in serum, suggesting that clioquinol also functions as a zinc ionophore in the human body.

The mechanisms by which clioquinol induces the oxidation of ATOX1 currently remain unclear. A previous study reported that clioquinol induced oxidative stress by

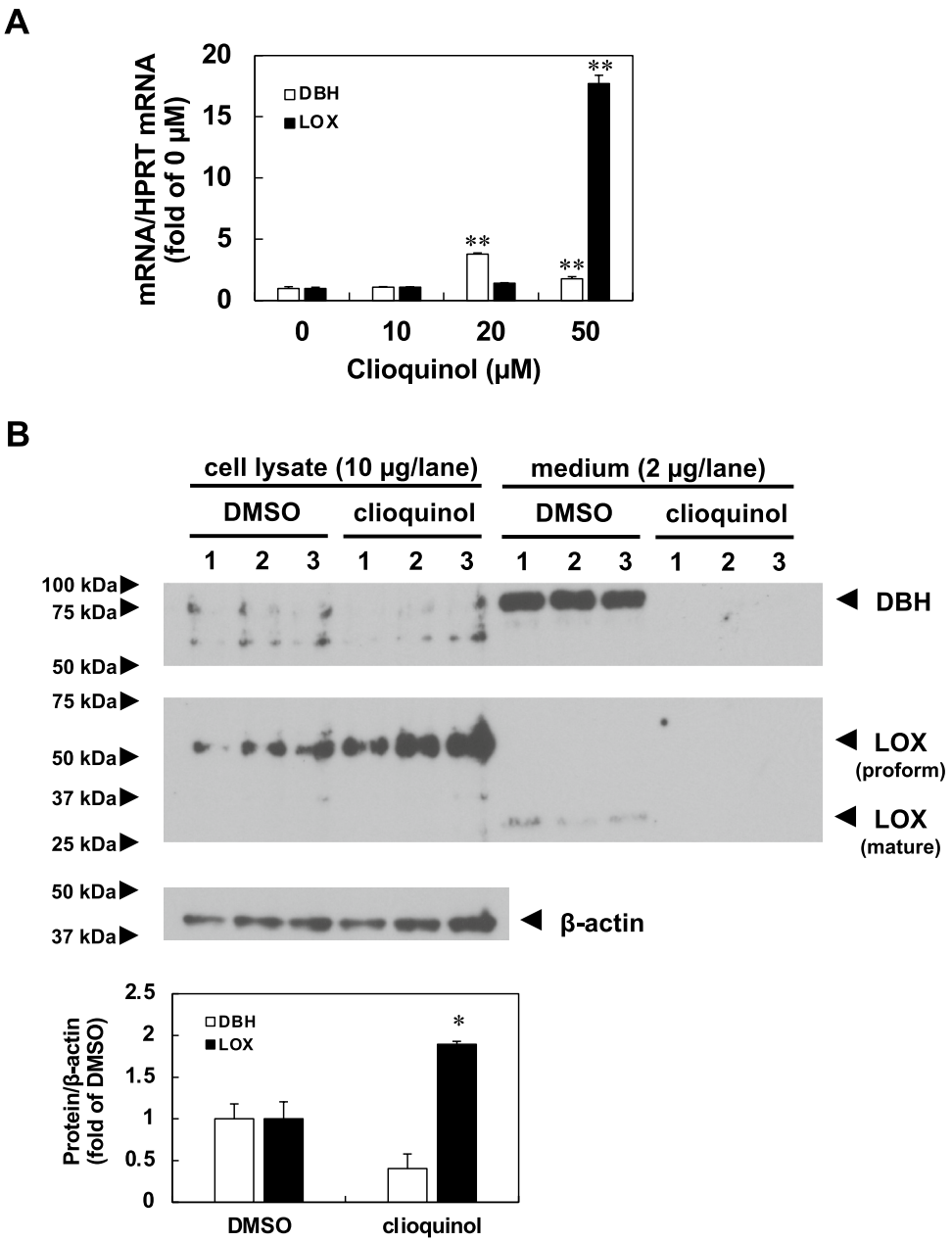

Fig. 4 Clioquinol inhibited the secretion of copper ectoenzymes and reduced the cellular level of NA. Cells were cultured in the presence or absence of clioquinol for 24 h. After washing with PBS, cells were cultured for 8 h with serum-free media containing the same concentrations of clioquinol. Media were concentrated and desalted using a centrifugal filter. Western blotting was performed as described in "Materials and methods" section. **a** Clioquinol increased the expression of mRNA for dopamine-β-hydroxylase (DBH) and lysyl oxidase (LOX). Bars represent the means ± SE of three individual wells. $^{**}p < 0.01$ vs. 0 μM. **b** Clioquinol (50 μM) inhibited the secretion of DBH and LOX. Samples (cell lysates and media) were prepared from three individual dishes. Quantitation results using ImageJ software are shown as a graph. Open bar, DBH. Closed bar, LOX. $^{*}p < 0.05$ vs. DMSO. **c** Dose-dependent suppression of DBH secretion by clioquinol. The experiment was repeated four times and representative results are shown. Quantitation results using ImageJ software are shown as a graph. $^{*}p < 0.05$, $^{**}p < 0.01$ vs. 0 μM. **d** Dose-dependent decrease in the intracellular level of NA by clioquinol. Bars represent the means ± SE of four individual wells. Open bar, undifferentiated cells. Closed bar, dbcAMP-induced differentiated cells. $^{**}p < 0.01$ vs. 0 μM

inhibiting SOD1, which may be due to the chelation of copper and/or zinc from SOD1 by clioquinol (Kawamura et al. 2014). Furthermore, it currently remains unclear whether the clioquinol-induced influx of zinc affects the activity of ATOX1. Metallothioneins induced by zinc influx were suggested to capture cytosolic copper and inhibit its binding to ATOX1. Zinc itself may also affect the activity of ATOX1. In a previous study using recombinant proteins, Zn^{2+} at concentrations lower than Cu^{+} mediated stable complex formation between ATOX1 and ATP7B by binding to cysteine residues in the metal-binding motifs of these proteins (van Dongen et al. 2006). The interaction between ATOX1 and ATP7A mediated by Zn^{2+} was ~ 200-fold stronger than that by Cu^{+} (Badarau et al. 2013). Thus, clioquinol-induced zinc influx may inhibit the copper-transporting activity of ATOX1 by competing with copper.

In the present study, the secretion of DBH into media was suppressed by the genome editing of ATOX1; however, this inhibition was weaker than that by clioquinol. Glutaredoxin-1 (Grx1) was previously reported to transfer copper to ATP7B in the absence of ATOX1, suggesting an alternative pathway in copper transport (Maghool et al. 2020). Clioquinol may affect the redox status of metal-binding domain-containing proteins, such as Grx1, ATP7A, and ATP7B, in addition to ATOX1, thereby blocking copper transport to copper-dependent enzymes.

Fig. 4 (continued)

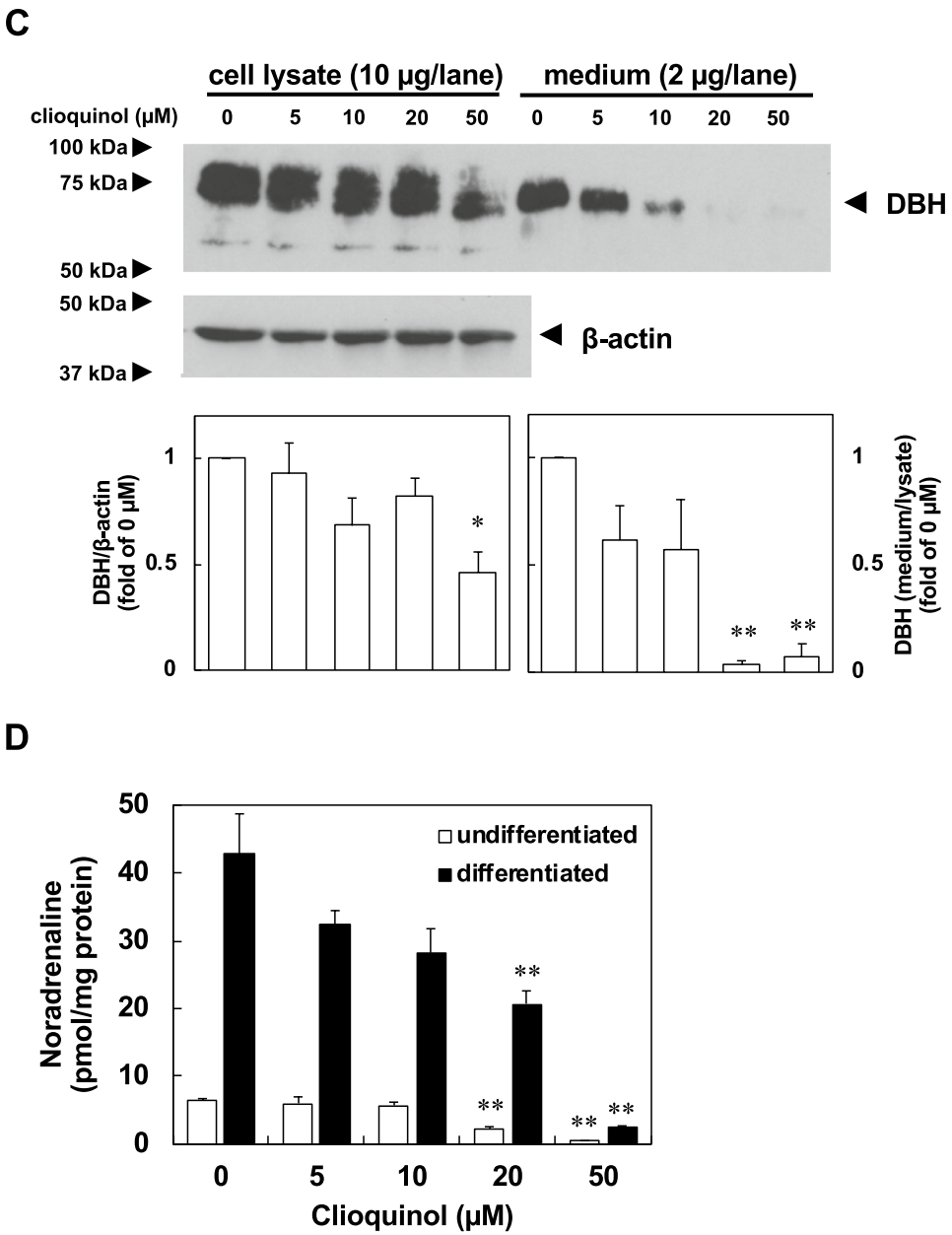

DBH is a key enzyme in the biosynthesis of NA, the neurotransmitter released from sympathetic postganglionic nerve fibers. DBH is targeted from the TGN to secretory granules, and secreted constitutively or by neuronal activation. Copper transport by ATP7A on the TGN is essential for functional maturation of DBH (Schmidt et al. 2018). Inhibition of the functional maturation of DBH and NA biosynthesis by clioquinol may lead to disturbances in the autonomic nervous system in SMON patients. Severe abdominal pain was previously reported after the administration of clioquinol and preceded the neurological symptoms of SMON (Meade 1975; Tateishi 2000). Clioquinol may elicit dominant parasympathetic nerve activity and subsequent intestinal hypercontraction. Descending noradrenergic projections from the locus coeruleus in the pontine to the dorsal horn of the spinal cord are known as the descending pain inhibitory system (Hayashida and Obata 2019). Disturbances in NA biosynthesis may affect the analgesic effects of the descending noradrenergic inhibitory system, leading to the characteristic dysesthesia of SMON.

LOX catalyzes the cross-linking of collagen and elastin, which form elastic fibers. LOX, synthesized as a 50-kDa precursor, is secreted and processed to a C-terminal 32-kDa mature enzyme and N-terminal 18-kDa propeptide without enzymatic activity (Trackman et al. 1992). The clioquinol-induced expression of LOX mRNA may be mediated by hypoxia-inducible factor (HIF)-1α because the *LOX* gene is a target of HIF-1α (Pez et al. 2011), which was reported to

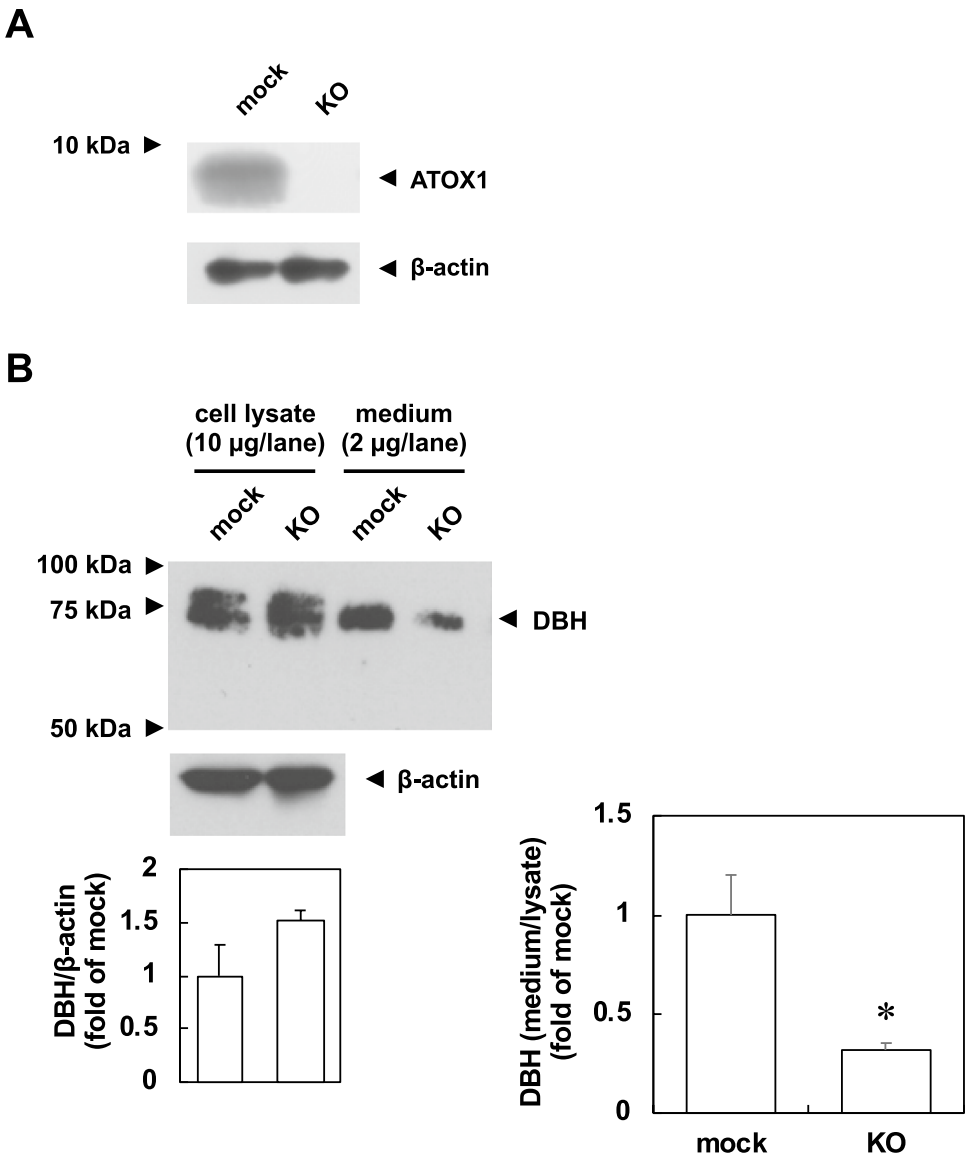

Fig. 5 Genome editing of ATOX1 suppressed the secretion of DBH. Western blotting was performed as described in "Materials and methods" section. **a** Gene disruption of ATOX1 in SH-SY5Y cells stably expressing guide RNA against ATOX1 (KO). **b** Suppression of DBH secretion in ATOX1-KO cells. The experiment was repeated three times and representative results are shown. Quantitation results using ImageJ software are shown as a graph. $*p < 0.05$ vs. mock

be stabilized by clioquinol through the inhibition of ubiquitination and asparagine hydroxylation (Choi et al. 2006). Regarding neuronal expression, LOX expression was previously reported to be up-regulated in the spinal cord of patients with amyotrophic lateral sclerosis (ALS) (Malaspina et al. 2001) and a G93A SOD1 transgenic mouse model of ALS (Li et al. 2004). A previous study reported that excess LOX propeptide suppressed Purkinje cell dendritic arborization (Li et al. 2010). Thus, clioquinol-induced alterations in the expression and secretion of LOX may affect essential neuronal functions. Further analyses are needed for a more detailed understanding of the relationship between the clioquinol-induced accumulation of the LOX proenzyme and clinical symptoms of SMON.

In conclusion, clioquinol-induced zinc influx, copper accumulation, and ATOX1 oxidation may impair the functional maturation of copper-dependent enzymes, such as DBH, leading to the inhibition of NA biosynthesis. This pathway may function, at least in part, in clioquinol-induced neurotoxicity.

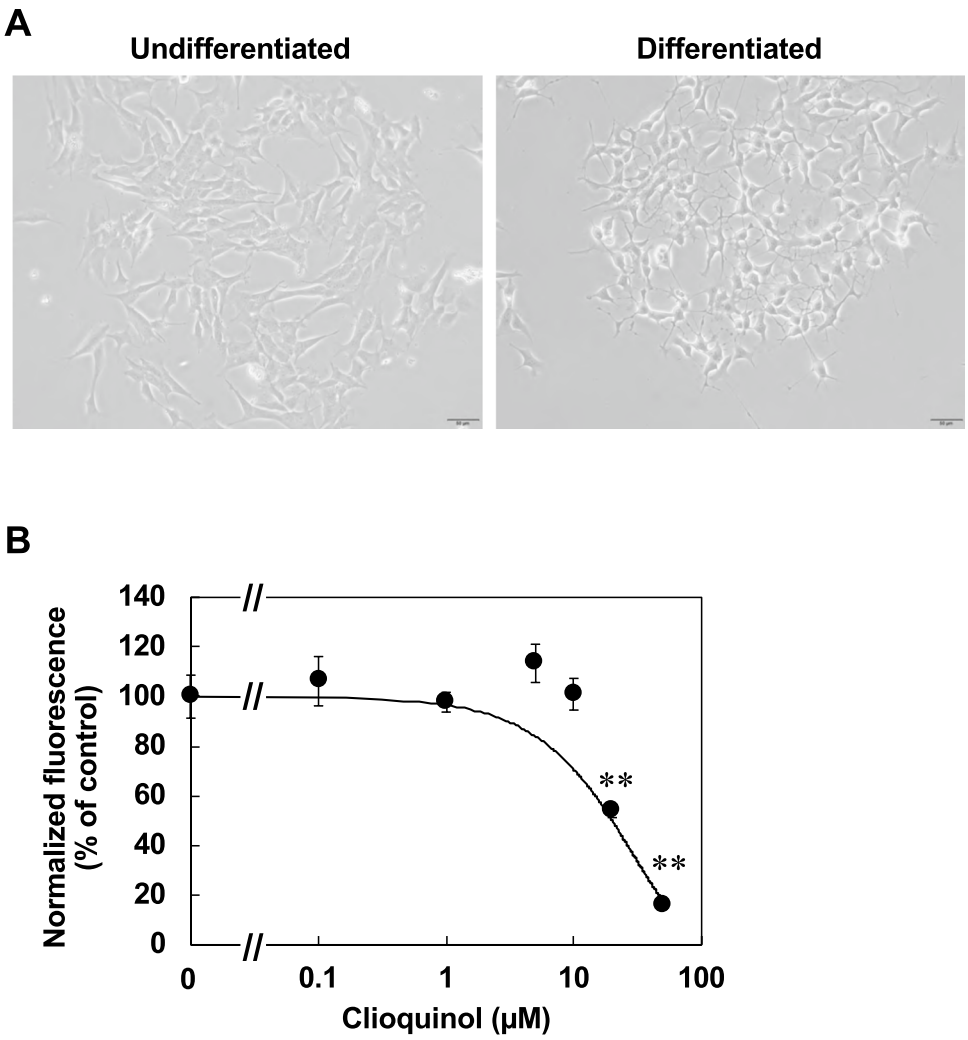

Fig. 6 Cytotoxic effects of clioquinol on dbcAMP-induced differentiated SH-SY5Y cells. **a** Morphological changes in SH-SY5Y cells induced by dbcAMP. Undifferentiated cells were cultured in Ham's F12: Eagle's medium with Earle's salts (1:1) supplemented with non-essential amino acids and 15% FBS. Differentiated cells were cultured for 3 days in Neurobasal medium containing B-27 supplement minus antioxidant and 1 mM dbcAMP. **b** Cytotoxic effects of clioquinol on differentiated cells. SH-SY5Y cells were seeded at 4000 cells/well and grown in 96-well plates for 24 h. Differentiation was induced as described in "Materials and methods" section. Cell viability at 24 h after clioquinol treatment was examined as described previously (Katsuyama et al. 2012). Bars represent the means ± SE of six individual wells. $^{**}p < 0.01$ vs. 0 μM

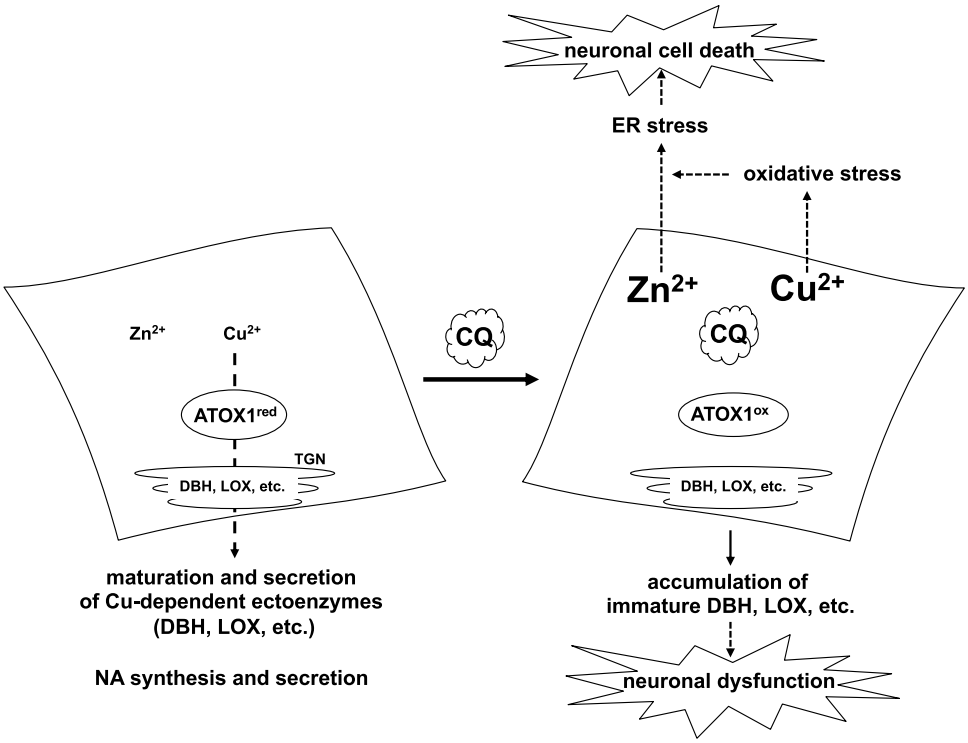

Fig. 7 Proposed mechanisms of clioquinol-induced neurotoxicity involving zinc influx and copper accumulation. CQ, clioquinol. TGN, trans-Golgi network

Acknowledgements This study was supported, in part, by a Health and Labor Sciences Research Grant for Research on Intractable Diseases from The Ministry of Health, Labour and Welfare of Japan (Grant no. H29-Intractable etc. (Intractable)-Designated-001).

Compliance with ethical standards

Conflict of interest The authors have no conflicts of interest to disclose with respect to this study.

Ethical standards This manuscript does not involve clinical studies or contain patient data.

References

Andersson DA, Gentry C, Moss S, Bevan S (2009) Clioquinol and pyrithione activate TRPA1 by increasing intracellular Zn2+. Proc Natl Acad Sci USA 106(20):8374–8379. https://doi.org/10.1073/pnas.0812675106

Asakura K, Ueda A, Kawamura N, Ueda M, Mihara T, Mutoh T (2009) Clioquinol inhibits NGF-induced Trk autophosphorylation and neurite outgrowth in PC12 cells. Brain Res 1301:110–115. https://doi.org/10.1016/j.brainres.2009.09.011

Badarau A, Basle A, Firbank SJ, Dennison C (2013) Crosstalk between Cu(I) and Zn(II) homeostasis via Atx1 and cognate domains. Chem Commun (Camb) 49(73):8000–8002. https://doi.org/10.1039/c3cc42709a

Bareggi SR, Cornelli U (2012) Clioquinol: review of its mechanisms of action and clinical uses in neurodegenerative disorders. CNS Neurosci Ther 18(1):41–46. https://doi.org/10.1111/j.1755-5949.2010.00231.x

Benvenisti-Zarom L, Chen J, Regan RF (2005) The oxidative neurotoxicity of clioquinol. Neuropharmacology 49(5):687–694. https://doi.org/10.1016/j.neuropharm.2005.04.023

Cater MA, Haupt Y (2011) Clioquinol induces cytoplasmic clearance of the X-linked inhibitor of apoptosis protein (XIAP): therapeutic indication for prostate cancer. Biochem J 436(2):481–491. https://doi.org/10.1042/BJ20110123

Cherny RA, Atwood CS, Xilinas ME et al (2001) Treatment with a copper-zinc chelator markedly and rapidly inhibits beta-amyloid accumulation in Alzheimer's disease transgenic mice. Neuron 30(3):665–676. https://doi.org/10.1016/s0896-6273(01)00317-8

Cheung YT, Lau WK, Yu MS et al (2009) Effects of all-trans-retinoic acid on human SH-SY5Y neuroblastoma as in vitro model in neurotoxicity research. Neurotoxicology 30(1):127–135. https://doi.org/10.1016/j.neuro.2008.11.001

Choi SM, Choi KO, Park YK, Cho H, Yang EG, Park H (2006) Clioquinol, a Cu(II)/Zn(II) chelator, inhibits both ubiquitination and asparagine hydroxylation of hypoxia-inducible factor-1alpha, leading to expression of vascular endothelial growth factor and erythropoietin in normoxic cells. J Biol Chem 281(45):34056–34063. https://doi.org/10.1074/jbc.M603913200

Ding WQ, Liu B, Vaught JL, Yamauchi H, Lind SE (2005) Anticancer activity of the antibiotic clioquinol. Cancer Res 65(8):3389–3395. https://doi.org/10.1158/0008-5472.CAN-04-3577

Egashira Y, Matsuyama H (1982) Subacute myelo-optico-neuropathy (SMON) in Japan. With special reference to the autopsy cases. Acta Pathologica Japonica 32(Suppl 1):101–116

Faux NG, Ritchie CW, Gunn A et al (2010) PBT2 rapidly improves cognition in Alzheimer's Disease: additional phase II analyses. J Alzheimers Dis 20(2):509–516. https://doi.org/10.3233/JAD-2010-1390

Finkelstein DI, Billings JL, Adlard PA et al (2017) The novel compound PBT434 prevents iron mediated neurodegeneration and alpha-synuclein toxicity in multiple models of Parkinson's disease. Acta Neuropathol Commun 5(1):53. https://doi.org/10.1186/s40478-017-0456-2

Fukui T, Asakura K, Hikichi C et al (2015) Histone deacetylase inhibitor attenuates neurotoxicity of clioquinol in PC12 cells. Toxicology 331:112–118. https://doi.org/10.1016/j.tox.2015.01.013

Geiser J, De Lisle RC, Finkelstein D, Adlard PA, Bush AI, Andrews GK (2013) Clioquinol synergistically augments rescue by zinc supplementation in a mouse model of acrodermatitis enteropathica. PLoS ONE 8(8):e72543. https://doi.org/10.1371/journal.pone.0072543

Grzywacz A, Gdula-Argasinska J, Muszynska B, Tyszka-Czochara M, Librowski T, Opoka W (2015) Metal responsive transcription factor 1 (MTF-1) regulates zinc dependent cellular processes at the molecular level. Acta Biochim Pol 62(3):491–498. https://doi.org/10.18388/abp.2015_1038

Hatori Y, Yan Y, Schmidt K et al (2016) Neuronal differentiation is associated with a redox-regulated increase of copper flow to the secretory pathway. Nat Commun 7:10640. https://doi.org/10.1038/ncomms10640

Hayashida KI, Obata H (2019) Strategies to treat chronic pain and strengthen impaired descending noradrenergic inhibitory system. Int J Mol Sci. https://doi.org/10.3390/ijms20040822

Hedera P, Fink JK, Bockenstedt PL, Brewer GJ (2003) Myelopolyneuropathy and pancytopenia due to copper deficiency and high zinc levels of unknown origin: further support for existence of a new zinc overload syndrome. Arch Neurol 60(9):1303–1306. https://doi.org/10.1001/archneur.60.9.1303

Hedera P, Peltier A, Fink JK, Wilcock S, London Z, Brewer GJ (2009) Myelopolyneuropathy and pancytopenia due to copper deficiency and high zinc levels of unknown origin II. The denture cream is a primary source of excessive zinc. Neurotoxicology 30(6):996–999. https://doi.org/10.1016/j.neuro.2009.08.008

Jack DB, Riess W (1973) Pharmacokinetics of iodochlorhydroxyquin in man. J Pharm Sci 62(12):1929–1932. https://doi.org/10.1002/jps.2600621204

Katsuyama M, Iwata K, Ibi M, Matsuno K, Matsumoto M, Yabe-Nishimura C (2012) Clioquinol induces DNA double-strand breaks, activation of ATM, and subsequent activation of p53 signaling. Toxicology 299(1):55–59. https://doi.org/10.1016/j.tox.2012.05.013

Katsuyama M, Ibi M, Matsumoto M, Iwata K, Ohshima Y, Yabe-Nishimura C (2014) Clioquinol increases the expression of VGF, a neuropeptide precursor, through induction of c-Fos expression. J Pharmacol Sci 124(4):427–432. https://doi.org/10.1254/jphs.13271fp

Katsuyama M, Ibi M, Iwata K, Matsumoto M, Yabe-Nishimura C (2018) Clioquinol increases the expression of interleukin-8 by down-regulating GATA-2 and GATA-3. Neurotoxicology 67:296–304. https://doi.org/10.1016/j.neuro.2018.06.014

Kawamura K, Kuroda Y, Sogo M, Fujimoto M, Inui T, Mitsui T (2014) Superoxide dismutase as a target of clioquinol-induced neurotoxicity. Biochem Biophys Res Commun 452(1):181–185. https://doi.org/10.1016/j.bbrc.2014.04.067

Kelner GS, Lee M, Clark ME et al (2000) The copper transport protein Atox1 promotes neuronal survival. J Biol Chem 275(1):580–584. https://doi.org/10.1074/jbc.275.1.580

Kimura E, Hirano T, Yamashita S et al (2011) Cervical MRI of subacute myelo-optico-neuropathy. Spinal Cord 49(2):182–185. https://doi.org/10.1038/sc.2010.68

Kume T, Kawato Y, Osakada F et al (2008) Dibutyryl cyclic AMP induces differentiation of human neuroblastoma SH-SY5Y cells into a noradrenergic phenotype. Neurosci Lett 443(3):199–203. https://doi.org/10.1016/j.neulet.2008.07.079

Kury S, Dreno B, Bezieau S et al (2002) Identification of SLC39A4, a gene involved in acrodermatitis enteropathica. Nat Genet 31(3):239–240. https://doi.org/10.1038/ng913

Langmade SJ, Ravindra R, Daniels PJ, Andrews GK (2000) The transcription factor MTF-1 mediates metal regulation of the mouse ZnT1 gene. J Biol Chem 275(44):34803–34809. https://doi.org/10.1074/jbc.M007339200

Lannfelt L, Blennow K, Zetterberg H et al (2008) Safety, efficacy, and biomarker findings of PBT2 in targeting Abeta as a modifying therapy for Alzheimer's disease: a phase IIa, double-blind, randomised, placebo-controlled trial. Lancet Neurol 7(9):779–786. https://doi.org/10.1016/S1474-4422(08)70167-4

Li PA, He Q, Cao T et al (2004) Up-regulation and altered distribution of lysyl oxidase in the central nervous system of mutant SOD1 transgenic mouse model of amyotrophic lateral sclerosis. Brain Res Mol Brain Res 120(2):115–122. https://doi.org/10.1016/j.molbrainres.2003.10.013

Li J, Gu X, Ma Y et al (2010) Nna1 mediates Purkinje cell dendritic development via lysyl oxidase propeptide and NF-kappaB signaling. Neuron 68(1):45–60. https://doi.org/10.1016/j.neuron.2010.08.013

Lin SJ, Culotta VC (1995) The ATX1 gene of Saccharomyces cerevisiae encodes a small metal homeostasis factor that protects cells against reactive oxygen toxicity. Proc Natl Acad Sci USA 92(9):3784–3788. https://doi.org/10.1073/pnas.92.9.3784

Maghool S, Fontaine S, Roberts BR, Kwan AH, Maher MJ (2020) Human glutaredoxin-1 can transfer copper to isolated metal binding domains of the P1B-type ATPase, ATP7B. Sci Rep 10(1):4157. https://doi.org/10.1038/s41598-020-60953-z

Malaspina A, Kaushik N, de Belleroche J (2001) Differential expression of 14 genes in amyotrophic lateral sclerosis spinal cord detected using gridded cDNA arrays. J Neurochem 77(1):132–145. https://doi.org/10.1046/j.1471-4159.2001.t01-1-00231.x

Mao X, Li X, Sprangers R et al (2009) Clioquinol inhibits the proteasome and displays preclinical activity in leukemia and myeloma. Leukemia 23(3):585–590. https://doi.org/10.1038/leu.2008.232

Matsuki Y, Ito T, Fukuhara K, Abe M, Othaki T, Nambara T (1987) Determination of chinoform in biological fluids and nervous tissues of the dog by gas chromatography-mass spectrometry. Arch Toxicol 59(5):374–378. https://doi.org/10.1007/bf00295093

Meade TW (1975) Subacute myelo-optic neuropathy and clioquinol. An epidemiological case-history for diagnosis. Br J Prev Soc Med 29(3):157–169. https://doi.org/10.1136/jech.29.3.157

Nakae K, Yamamoto S, Shigematsu I, Kono R (1973) Relation between subacute myelo-optic neuropathy (S.M.O.N.) and clioquinol: nationwide survey. Lancet 1(7796):171–173. https://doi.org/10.1016/s0140-6736(73)90004-4

Nations SP, Boyer PJ, Love LA et al (2008) Denture cream: an unusual source of excess zinc, leading to hypocupremia and neurologic disease. Neurology 71(9):639–643. https://doi.org/10.1212/01.wnl.0000312375.79881.94

Pez F, Dayan F, Durivault J et al (2011) The HIF-1-inducible lysyl oxidase activates HIF-1 via the Akt pathway in a positive regulation loop and synergizes with HIF-1 in promoting tumor cell growth. Cancer Res 71(5):1647–1657. https://doi.org/10.1158/0008-5472.CAN-10-1516

Ritchie CW, Bush AI, Mackinnon A et al (2003) Metal-protein attenuation with iodochlorhydroxyquin (clioquinol) targeting Abeta amyloid deposition and toxicity in Alzheimer disease: a pilot phase 2 clinical trial. Arch Neurol 60(12):1685–1691. https://doi.org/10.1001/archneur.60.12.1685

Schmidt K, Ralle M, Schaffer T et al (2018) ATP7A and ATP7B copper transporters have distinct functions in the regulation of neuronal dopamine-beta-hydroxylase. J Biol Chem 293(52):20085–20098. https://doi.org/10.1074/jbc.RA118.004889

Spinazzi M, De Lazzari F, Tavolato B, Angelini C, Manara R, Armani M (2007) Myelo-optico-neuropathy in copper deficiency occurring after partial gastrectomy. Do small bowel bacterial overgrowth syndrome and occult zinc ingestion tip the balance? J Neurol 254(8):1012–1017. https://doi.org/10.1007/s00415-006-0479-2

Sturtevant FM (1980) Zinc deficiency, acrodermatitis enteropathica, optic atrophy, subacute myelo-optic neuropathy, and 5,7-dihalo-8-quinolinols. Pediatrics 65(3):610–613

Tanaka KI, Shimoda M, Kasai M, Ikeda M, Ishima Y, Kawahara M (2019) Involvement of SAPK/JNK signaling pathway in copper enhanced zinc-induced neuronal cell death. Toxicol Sci 169(1):293–302. https://doi.org/10.1093/toxsci/kfz043

Tateishi J (2000) Subacute myelo-optico-neuropathy: clioquinol intoxication in humans and animals. Neuropathology 20(Suppl):S20–S24. https://doi.org/10.1046/j.1440-1789.2000.00296.x

Trackman PC, Bedell-Hogan D, Tang J, Kagan HM (1992) Post-translational glycosylation and proteolytic processing of a lysyl oxidase precursor. J Biol Chem 267(12):8666–8671

Tsubaki T, Honma Y, Hoshi M (1971) Neurological syndrome associated with clioquinol. Lancet 1(7701):696–697. https://doi.org/10.1016/s0140-6736(71)92699-7

van Dongen EM, Dekkers LM, Spijker K, Meijer EW, Klomp LW, Merkx M (2006) Ratiometric fluorescent sensor proteins with subnanomolar affinity for Zn(II) based on copper chaperone domains. J Am Chem Soc 128(33):10754–10762. https://doi.org/10.1021/ja0610030

Xie HR, Hu LS, Li GY (2010) SH-SY5Y human neuroblastoma cell line: in vitro cell model of dopaminergic neurons in Parkinson's disease. Chin Med J 123(8):1086–1092